

appeared possible that the transitions measuring the low-spin crystal field were shifted to lower energy. This shift from low spin to high spin with increasing pressure at first appears paradoxical. One knows that the ligand field in high-spin complexes increases with decreasing metal-ligand distance.¹ There is a critical value of Δ of about 14 000–15 000 cm^{-1} , wherein a transition from high spin to low spin is expected. This has been observed as a function of temperature¹⁵ and in this laboratory as a function of pressure in phenanthroline complexes.¹⁶

However, the conversion of Fe(III) to Fe(II) with pressure indicates that iron has an increased affinity for electrons with increasing compression, and that the 3d levels lower in energy with respect to the ligand levels. These factors would tend to reduce the back donation and weaken the pi bonding, increasing the energy of the low-spin state. The situation is illustrated schematically

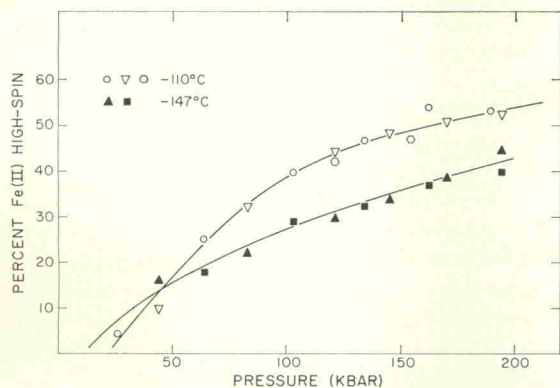


Fig. 9. Conversion to high-spin Fe(II) at 110°C and 147°C—copper ferricyanide.

in Fig. 6. Movement to the left in the figure represents increasing Δ and decreasing R (Fe-C distance). The decreased back donation has the effect of moving the low-spin potential well up, and possibly to the right. The high-spin potential well moves to left, until one arrives at a state where electrons can transfer thermally from the low-spin to the high-spin state. It is clear that high-pressure-high-temperature optical studies would be very helpful. The combined temperature-pressure wavelength range is beyond the reach of our old single-beam high-pressure optical apparatus, but a double-beam system is being developed, and eventually such measurements should be possible.

The dependence of conversion on the cation is of interest. It is consistent with the isomer-shift data of Fig. 1. The K^+ and Na^+ salts which showed no conversion exhibit large decreases in isomer shift due to increased sigma bonding. In the Cu^{+2} salt the increased

¹⁵ E. König and K. Madeja, *Inorg. Chem.* **6**, 48 (1967).

¹⁶ D. C. Fisher (personal communication, 1968).

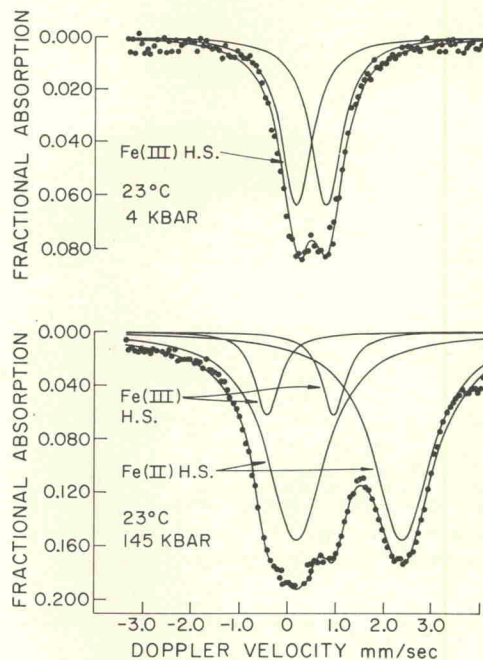


Fig. 10. Mössbauer spectra of $\text{Fe}_{47}[\text{Fe}(\text{CN})_6]_3$.

shielding due to decreased back bonding actually overcomes the first effect. The other salts are intermediate. The order of electronegativity as determined from electrode potentials is $\text{K} > \text{Na} > \text{Zn} > \text{Ni} > \text{Cu}$. Evidently the metal with the greatest tendency for covalency has the greatest effect in decreasing back donation. The difference in crystal structure between heavy metal and alkali salts may also be a factor. The possibility exists

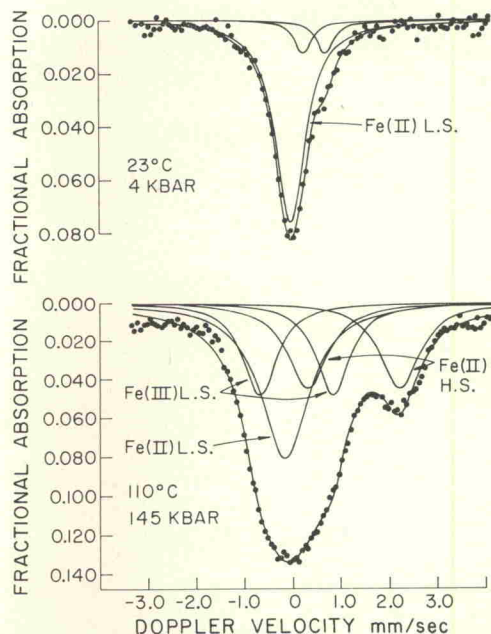


Fig. 11. Mössbauer spectra of $\text{Fe}_4[\text{Fe}^{57}(\text{CN})_6]_3$.

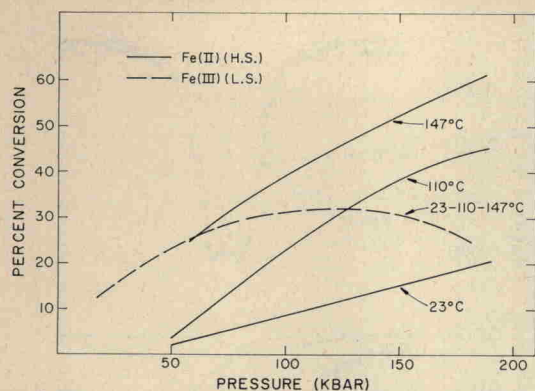


FIG. 12. Conversion to low-spin Fe(III) and high-spin Fe(II) vs pressure— $\text{Fe}_4[^{57}\text{Fe}(\text{CN})_6]_3$.

that one is observing isomerization, i.e., that the cyanide ion is flipping so that the nitrogen bonds to the iron. The prussian-blue spectra discussed later in this paper, and the spectra of $\text{Fe}^{57}\text{Fe}(\text{CN})_5\text{NO}$ discussed in the following paper effectively eliminate this possibility.

FERRICYANIDES

The ferricyanides of the same five cations were studied in high pressure and high temperature. In a previous paper⁹ we showed that $\text{K}_3\text{Fe}(\text{CN})_6$ reduced to the ferrous state very rapidly with increasing pressure at room temperature until a first-order phase transition intervened. All of the other four salts also reduced very rapidly with pressure at 23°C but with no sign of a phase transition. The ferrous and ferric isomer shifts are superimposed, and only in the sodium salt could we get any quantitative measure of the amount of reduction. The quadrupole splitting of the ferric ion in the heavy metal salts was too small to permit a fit to be made. The initial isomer shifts are listed in Table III. The reduction of sodium ferricyanide could be described by the relation

$$K = C_{\text{II}}/C_{\text{III}} = 0.12P^{1.57}, \quad (1)$$

where C_{II} and C_{III} are the concentrations of ferrous

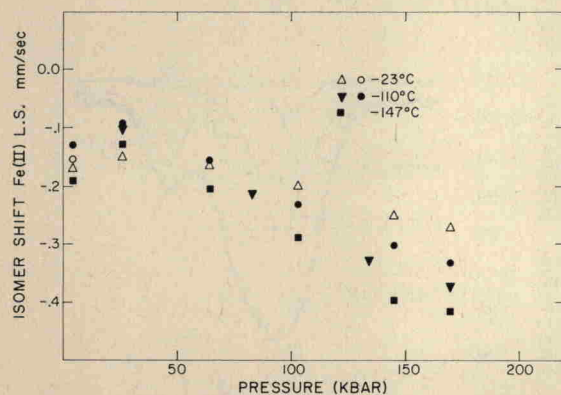


FIG. 13. Isomer shift vs pressure—low-spin Fe(II) in $\text{Fe}_4[^{57}\text{Fe}(\text{CN})_6]_3$.

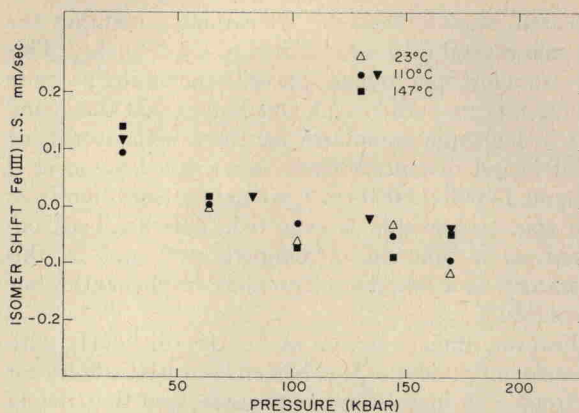


FIG. 14. Isomer shift vs pressure—low-spin Fe(III) in $\text{Fe}_4[^{57}\text{Fe}(\text{CN})_6]_3$.

and ferric sites with their ligands, and P is the pressure in kilobars. At 110°C and high pressure all of these materials exhibited high-spin Fe(II) peaks which increased in size with pressure. The isomer shifts were in the same range as for the ferrocyanides. The quadrupole splittings appear in Table IV. The conversions at 110°C are shown in Fig. 7. For every salt except the copper the conversion to high-spin Fe(II) is substantially higher than for the ferrocyanides. Even the K^+ and Na^+ salts show measurable conversion. There are some differences in crystal structure—the heavy metals involve both bridged and interstitial cations. However, we believe that the main difference is the following. At the reduction we have a low-spin Fe(II) surrounded by six $(\text{CN})^-$ ions plus a hole. This hole serves to weaken the bonding and move the low-spin potential well up and to the right in Fig. 6. Again, high-pressure optical studies will be helpful.

The $\text{Cu}_3[\text{Fe}(\text{CN})_6]_2$ ion exhibited an additional feature of interest. At 110°C it behaved like the other salts. At 147° and low pressure, before any significant reduction appeared, it exhibited considerable conversion of low-spin Fe(III) to high-spin Fe(III), as can be seen in the upper spectrum of Fig. 8. With increasing pressure the high-spin Fe(III) reduced to high-spin Fe(II) as in the lower spectrum. Figure 9 shows that the amount of high-spin Fe(II) at a given pressure was actually less at 147°C than at 110°C. The shape of the conversion-pressure curve is also different. The reduc-

TABLE V. Yield of high-spin Fe(II) from $^{57}\text{Fe}_4[\text{Fe}(\text{CN})_6]_3$.

Pressure (kbar)	Percent 23°C	Fe(II) H.S. 147°C
20	12	35
60	40	73
100	67	88
140	83	95
180	92	97